

Diverging Relaxation Times of Domain Wall Motion Indicating Glassy Dynamics in Ferroelastics

Sabine Puchberger^a, Viktor Soprunyuk^a, Wilfried Schranz^{a*} 

^aFaculty of Physics, University of Vienna, Vienna, Austria

Received: September 22, 2017; Revised: February 09, 2018; Accepted: April 20, 2018

Single crystals of PbZrO_3 and LaAlO_3 have been studied by Dynamic Mechanical Analysis measurements in the low frequency range $f = 0.02\text{-}50$ Hz. The complex Young's modulus exhibits a quite rich behavior and depends strongly on the direction of the applied dynamic force. The low frequency elastic response in the $[110]_c$ -direction is dominated by domain wall motion, leading to a superelastic softening effect below T_c . With decreasing temperature this superelastic softening gradually disappears, due to an increasing relaxation time τ_{DW} of domain wall motion. For PbZrO_3 , τ_{DW} seems to diverge at a finite temperature T_{VP} , indicating glassy behavior of domain freezing.

Keywords: domain wall motion, glass transition, dynamic mechanical analysis.

1. Introduction

Domain walls (DW's) can have a strong influence on the dielectric and elastic properties of materials. The contribution from the motion of domain walls leads to an increased macroscopic response as compared to single domain response and significant anelastic behavior. In ferroelastics the domain wall motion subject to external stress leads to so called "superelastic softening"^{1,2}. Superelastic softening has been observed in many ferroelastic materials, e.g. in SrTiO_3 ³, LaAlO_3 ^{4,5}, PbZrO_3 ⁶, $\text{Ca}_{1-x}\text{Sr}_x\text{TiO}_3$ ⁷, KMnF_3 ^{8,9} etc.

At finite measurement frequencies, the domain wall response can change drastically^{10,11}. In some cases, a freezing of the domain wall motion occurs at lower temperatures T_f where the domain walls can no longer follow the dynamically applied external force. As a result, the susceptibility falls down to a value corresponding to the domain-averaged limit. Prominent examples in which such a behavior was found in dielectric measurements are e.g. KDP^{12} (KH_2PO_4) and TGS^{13} ($(\text{NH}_2\text{CH}_2\text{COOH})_3 \cdot \text{H}_2\text{SO}_4$). In SrTiO_3 the domain wall contribution to the elastic susceptibility is largely exceeding the intrinsic (due to coupling between the order parameter and strain) elastic anomaly³. No domain wall freezing occurs down to the lowest measured $T = 6$ K in SrTiO_3 , whereas in most of the other studied ferroelastic materials domain wall freezing was observed at $T_f < T_c$.

A similarity of domain wall dynamics and glass behavior was already noticed some time ago in the ferroelectrics KDP and TGS^{14} . The authors proposed that pinning of randomly distributed defects to domain walls is responsible for the domain freezing process. To explain the measured diverging relaxation time the authors assumed that the pinning becomes increasingly collective at low temperatures. In other words,

the collective pinning energy $E_{\text{CP}} \rightarrow \infty$ for $T \rightarrow T_p$, thereby restricting the motion of DW's and leading to a Vogel-Fulcher (VF) type divergence of DW relaxation times.

In a recent paper, Kumar et al.¹⁵ reported an electric field-induced transition between locally pinned (rather strong glass-former) and clustered (super-fragile glass-former) phases of domain-wall-matter in KDP . Ren et al.^{16,17} reported "strain glass" behavior in TiNi -based alloys. The authors found a crossover from a normal martensitic transition to a strain glass behavior due to point defect doping in the $\text{Ti}_{50-x}\text{Ni}_{50+x}$ system around $x_c \sim 1.1$ where x is the concentration of point defects (excess Ni). Ren concluded that strain glass is the glass form of a ferroelastic/martensitic system due to point defect doping. He mentioned the striking similarity between strain glass and ferroelectric relaxor and cluster spin glass that leads to the concept of ferroic glass.

Very recently, Salje et al.^{18,19} proposed the existence of glasses in ferroelastic systems, appearing without the need for any defects, which led him to the concept of "domain glass". The basic idea²⁰ is that the domain boundaries can generate the defects intrinsically and, at a certain density of domain walls, jamming leads to a Vogel-Fulcher type slowing down of the dynamics around T_{VF} . The authors predicted the existence of two distinct regimes of DW movement: a low temperature athermal regime and a high temperature thermally activated regime. At higher temperatures, thermal activation leads to a Vogel-Fulcher distribution of avalanches. The slowing down of DW dynamics with decreasing temperature is reminiscent of glassy behavior. Below the VF temperature the DW's show jerky, athermal movements. Such intermittent response of a system to slowly changing external fields was also found in the context of ferromagnetic domain walls²¹⁻²³.

*e-mail: wilfried.schranz@univie.ac.at

The opportunity to study the physics of glasses in domain wall systems has lead to the present study of the movement of domain walls in PbZrO_3 and LaAlO_3 .

2. Experimental

The low frequency elastic measurements were performed with a Dynamic Mechanical Analyser (Diamond DMA, Perkin Elmer). We used "parallel plate geometry" (PP) where the sample is placed between two parallel plates and subject to a static force F_{stat} with an additional smaller dynamic force F_{dyn} whose frequency can be varied between $f=0.01$ -100 Hz. The DMA registers the amplitude u and phase shift δ between applied force and amplitude via a linear variable differential transformer (LVDT), which is used to calculate the real and imaginary part of the samples Young's modulus $Y^* = Y' + iY''$

$$Y^*(\vec{p}) = \frac{h}{u} \frac{F_{\text{dyn}}}{A} \exp i\delta \quad (1)$$

where h denotes the sample thickness, A its area and \vec{p} refers to the direction of the applied force, with respect to the crystal axes.

For samples we chose LaAlO_3 and PbZrO_3 , both perovskite single crystals. LaAlO_3 exhibits a phase transition at $T_c = 823$ K changing its crystal structure from cubic $Pm3m$ to rhombohedral $R3c$ ⁵. In PbZrO_3 the phase transition takes place at $T_c \sim 509$ K and results in a change from a paraelectric phase with cubic symmetry to an orthorhombic antiferroelectric $Pbam$ phase⁶. A typical domain structure of PbZrO_3 at room temperature is shown in Fig.1.

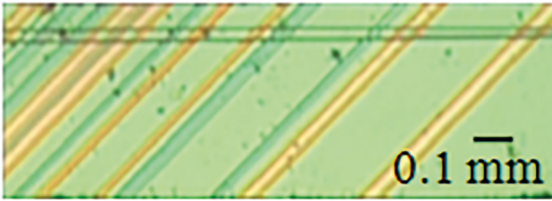


Figure 1. Typical ferroelastic domain pattern of PbZrO_3 single crystal observed at RT with a polarizing microscope under crossed polarizers.

The dimensions of the measured samples are approximately $A \approx 2$ mm², $h \approx 1.8$ mm for PbZrO_3 and $A \approx 1$ mm², $h \approx 2.5$ mm for LaAlO_3 . Concerning the measurement device, the resolution of DMA is $\Delta u \sim 10$ nm and $\Delta \delta \sim 0.1^\circ$. Although the relative accuracy of DMA measurements is within 0.2-1%, the absolute accuracy is usually not better than about 20%. For this reason all plots are shown here in terms of normalized Young's modulus $Y'_n = Y'/Y'_{\text{para}}$ and $Y''_n = Y''/Y'_n \tan(\delta)$, where Y'_{para} is the saturation value of the Young's modulus in the cubic phase. A more detailed description of the DMA method and its application for the study of phase transitions is given in Refs.²⁴ and²⁵.

3. Results

Temperature and frequency dependent DMA measurements of PbZrO_3 single crystals with forces applied in two different directions are presented in the following figures. Fig. 2 shows real and imaginary parts of the Young's modulus measured along one of the main cubic crystallographic axes. In the $[100]_c$ direction the force is perpendicular to the domain wall orientations and, as a result, the elastic anomaly resembles the intrinsic behavior. A pronounced softening of the elastic constant is already detected in the cubic phase, followed by a dip in Y' and a peak in Y'' at T_c . Both anomalies decrease with increasing frequency. This decrease of both anomalies with increasing frequency implies that $\omega\tau > 1$, leading to $\tau \sim 1$ s.

A quite different pattern is found (Fig.3) when the applied force is rotated by 45° to measure $Y_{[110]_c}$. Instead of the narrow dip in Y' of Fig. 2, a large softening is now detected in this direction which is accompanied by a broad peak in Y'' below T_c . With increasing frequency, the peak maximum of the broad peak shifts to higher temperatures.

It is evident that the low frequency elastic behavior in this direction is dominated by domain wall motion that results in the additional softening³. At sufficiently low frequencies the domain walls can follow the externally applied stress as long as the characteristic relaxation time τ_{DW} for DW movement is small enough, leading to superelastic softening. With decreasing temperature, τ_{DW} increases and the DW's can no longer follow the applied stress, implying that the elastic response returns to the domain averaged value.

To analyze the underlying dynamics in more detail, we have fitted the data of Y'' in the crossover region where $\omega\tau_{\text{DW}}(T) < 1 \rightarrow \omega\tau_{\text{DW}}(T) > 1$ using a Cole-Cole relaxation, i.e.

$$Y''(T) = Y_\infty + \frac{Y_0 - Y_\infty}{1 + (i\omega\tau_{\text{DW}})^{1-\alpha}} \quad (2)$$

where Y_∞ denotes the elastic compliance in the high frequency limit where $\tau_{\text{DW}} \gg 1$ and $\Delta Y^{\text{DW}} = Y_0 - Y_\infty$ refers to the DW-induced softening. The exponent $1-\alpha$ leads to a broadening (if $\alpha > 0$) of the Debye relaxation, which is obtained in the limit $\alpha = 0$. The Cole-Cole relaxation function fits the data quite well (Fig. 4), yielding $\alpha = 0.8$ for PbZrO_3 and $\alpha = 0.6$ for LaAlO_3 .

From the fits at various frequencies, we extracted the temperature dependencies of the relaxation times shown in Fig. 5.

The temperature dependence of DW relaxation time in PbZrO_3 can be well fitted with a Vogel-Fulcher law $\tau_{\text{DW}} = \tau_0 e^{\frac{E_a}{k_b(T-T_{\text{VF}})}}$ yielding an activation energy $E_a = 0.23 \pm 0.01$ eV, $\tau_0 = 1.2 \cdot 10^{-7}$ s and $T_{\text{VF}} = 120$ K. Although VF-behavior fits the data well, the low activation energy is difficult to rationalize. Thus we tried to fit the data with Arrhenius law, yielding $E_a = 0.58 \pm 0.02$ eV, $\tau_0 = 5.1 \cdot 10^{-11}$ s. For LaAlO_3 a clear Arrhenius behavior is observed with an activation energy $E_a = 1.02$ eV which is close to the values usually

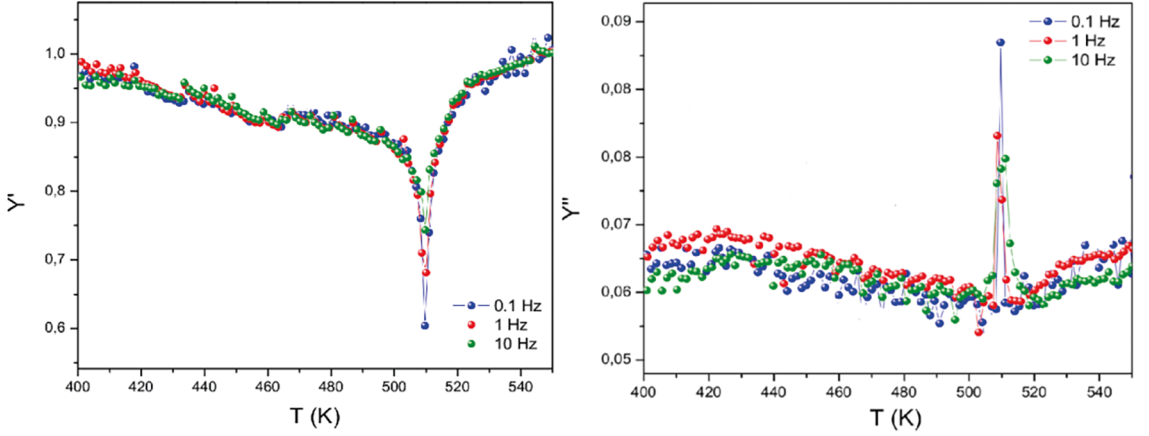


Figure 2. Temperature dependencies of real (left) and imaginary (right) parts of normalized Young's modulus of PbZrO_3 measured in the $[100]_c$ direction at various frequencies.

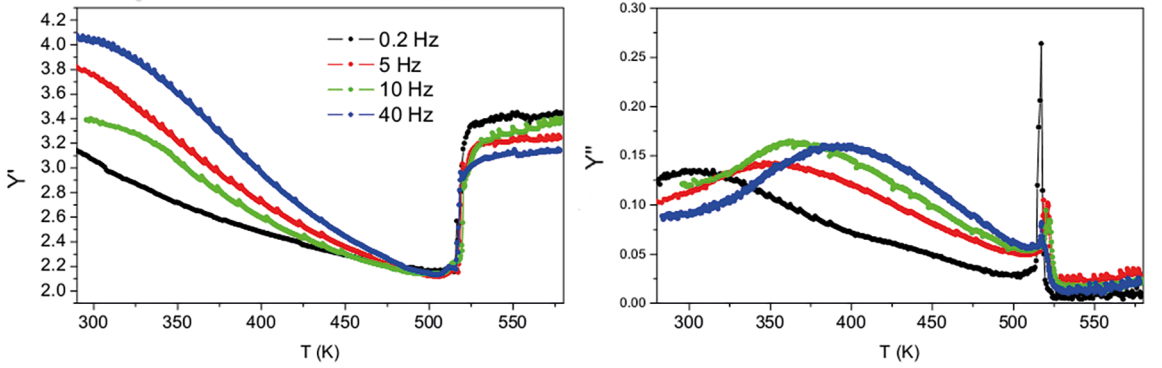


Figure 3. Temperature dependencies of real and imaginary parts of Young's modulus of PbZrO_3 measured in the $[110]_c$ direction at various frequencies.

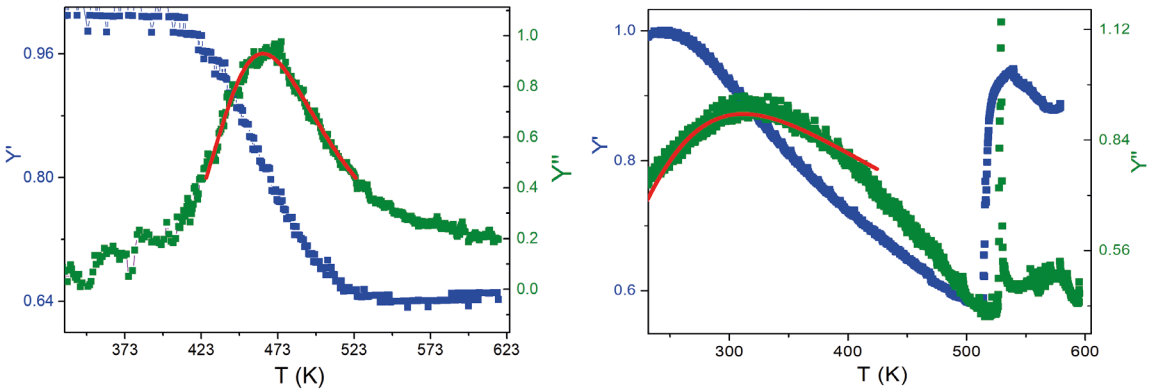


Figure 4. Real (blue) and imaginary (green) parts of the complex Young's modulus of PbZrO_3 (right) and LaAlO_3 (left) and corresponding Cole-Cole fits using equation (2).

found in perovskites and explained by pinning of DW's to oxygen defects⁴. For comparison, the activation energies in other perovskites have been determined to be $E_a = 0.309 \pm 0.004$ eV in BaCeO_3 ²⁶ and $E_a = 0.59 \pm 0.09$ eV in BiFeO_3 ²⁷.

To gain further insight into the domain wall motion processes, we investigated the sample's response at increasing

static stress with very low compression rates (3-15 mN/min). The propagation of elastic walls in an external stress field shares some similarities with the behavior of magnetic walls subject to an external magnetic field. The result of such measurements is shown in Fig. 6, depicting the discontinuous evolutions of the sample height.

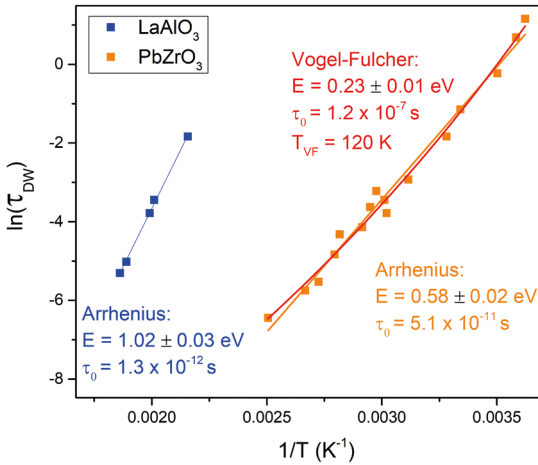


Figure 5. Arrhenius plots of domain wall relaxation times of LaAlO₃ and PbZrO₃.

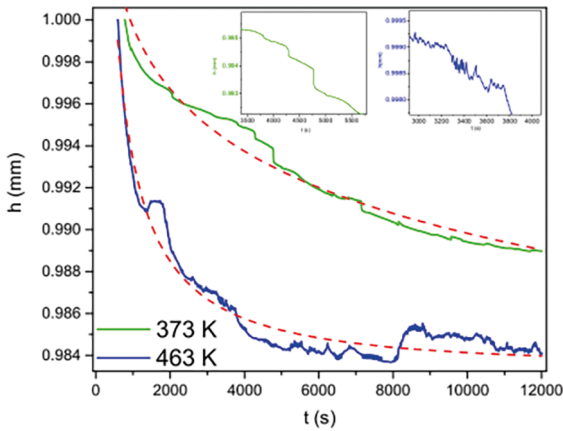


Figure 6. Height evolution during slow compression of PbZrO₃ at two different temperatures. The applied force is increased at a rate of 15 mN/min from 10 to 3000 mN. The dashed red lines correspond to (stretched)-exponential fits. Magnifications of $h(t)$ are shown in insets.

It can be seen that at low temperatures the height evolution follows a stretched-exponential relaxation envelope that is punctuated by jerks of varying amplitudes. These height drops are manifestations of pinning/depinning events of domain walls to defects or due to mutual jamming of the walls. Upon increasing the temperature, the height evolution changes considerably, which is also reflected in the squared drop velocity peaks (shown in Fig. 7) calculated from the height drops as $v^2 = (dh/dt)^2$.

At low temperatures, the squared drop velocity peaks vary over several orders of magnitude but their number increases gradually upon increasing temperature. This effect is due to thermal fluctuations which ease the motion of the domain walls, leading to a decrease of the DW relaxation time. To quantify this behavior in more detail, we have calculated the distributions of squared drop velocity maxima $N(v_m^2)$ from the height drops by binning the peak data logarithmically

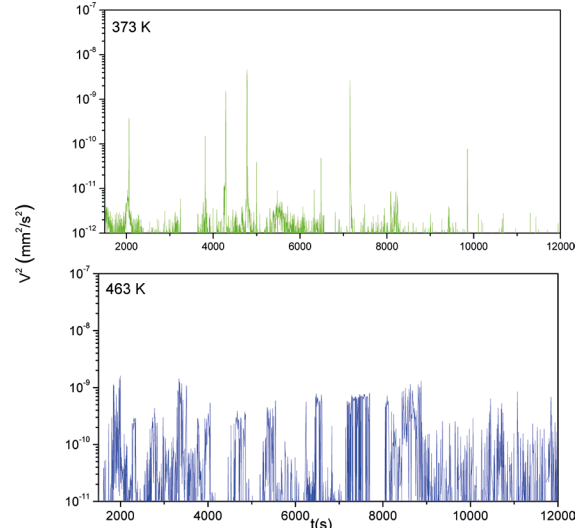


Figure 7. Squared drop velocity peaks $v_m^2 = (dh/dt)^2_{max}$ of PbZrO₃ at two different temperatures.

and plotting a histogram. Fig. 8 shows a log-log plot of the distributions of squared drop velocity maxima of the peak data of PbZrO₃ at different temperatures. In the low T region the curves are fitted according to a power law $N(v_m^2) \approx (v_m^2)^{-\epsilon}$, with exponent $\epsilon = 1.6 \pm 0.2$. At higher T the distribution changes from power-law to exponential, in good agreement with recent computer simulations²⁸.

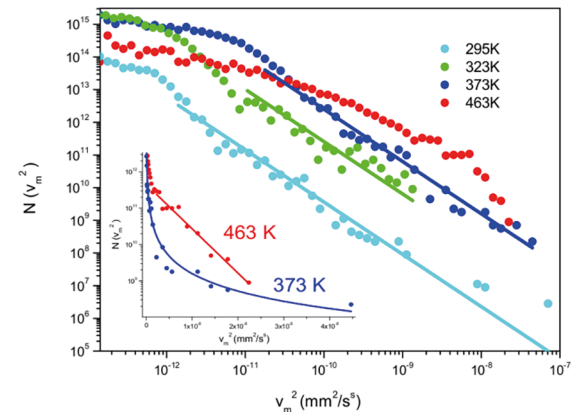


Figure 8. Log-log plot of the distribution $N(v_m^2)$ of maximum drop velocities squared of PbZrO₃ at different temperatures. Curves are shifted for clarity. The inset shows a log-linear plot of the curves at 373 K and 463 K.

4. Discussion

In single crystals of PbZrO₃ results show that, below T_c , there is a distinct dependence of the elastic response on the orientation of the applied stress. No domain wall motion is observed if dynamic forces are applied parallel or perpendicular to the domain walls. In directions 45° with respect to domain walls, we have detected an additional

contribution to the elastic behavior which is due to domain wall motion. This additional softening disappears gradually with decreasing temperature due to domain wall freezing at T_f . The domain wall dynamics are seen in the imaginary part of the complex Young's modulus as a broad peak around the domain freezing temperature T_f . From a detailed analysis of this peak and its shift with frequency we have determined the domain wall relaxation time τ_{DW} . Although a Vogel-Fulcher temperature dependence fits the data well, there are several points that should be considered. The obtained activation energy $E_a \sim 0.23$ eV cannot be rationalized straightforwardly. In addition, the Cole-Cole relaxation function, which yields an exponent of $\alpha = 0.8$, implies a distribution of relaxation times. As shown by Tagantsev²⁹ a gradual broadening of the relaxation time distribution with decreasing temperature could be mistaken for a VF type freezing of the system. From the present data we cannot exclude the possibility that such an effect of overlapping Debye peaks with different T-dependencies could mimic a VF-dependence of τ_{DW} in PbZrO_3 . We also tried to fit the temperature dependence of τ_{DW} with an Arrhenius law, yielding an energy barrier of $E_a \sim 0.58$ eV. This is slightly lower than the value usually found in perovskites for pinning of DW's to oxygen defects^{30,31}. However, as clearly seen in Fig. 5 the Arrhenius law fits the data less well, in comparison with the Vogel-Fulcher law, thus indicating a divergence of the domain wall relaxation time at $T_{VF} \approx 120$ K.

In glass-forming liquids³², it is well understood that the diverging relaxation time at finite temperature (T_{VF}) is due to the presence of dynamically correlated regions whose size ξ increases, reaching infinity at T_{VF} . It is a challenge to look for such dynamical correlations in systems with domain freezing. The present study shows that PbZrO_3 could be a good candidate for this purpose.

A clear Arrhenius behavior with energy barrier $E_a \sim 1.02$ eV is observed in LaAlO_3 and it is settled that a pinning of domain walls to defects (e.g. oxygen vacancies) is the main reason for the increasing domain wall relaxation time with decreasing temperature. These pinning effects are also clearly observed as strain drops of samples measured under slowly increasing external stress. The value of the exponent obtained from fitting the squared drop velocity distributions corresponds well with the value found by Harrison et al.³³ who obtained $\epsilon = 1.8 \pm 0.2$ for the jerky propagation of a single ferroelastic needle domain in LaAlO_3 under weak external stress at the critical depinning threshold of domain walls. These authors observed discrete jumps of the needle tip of varying amplitude due to pinning/depinning of wall segments to defects and described the movement of a needle domain as a superposition of a smooth front propagation and a stop-and-go propagation of the needle tip. The present results support the view of domain wall motion in a multidomain system as having similar characteristics to a single domain wall.

A very similar jerky propagation of domain walls under slowly increasing external stress was also observed in PbZrO_3 . The crossover which is observed in the squared drop velocity peaks with increasing temperature, Fig. 6, is also reflected in the squared drop velocity distributions, Fig. 8. In PbZrO_3 a power law behavior of $N(v_m^{-2})$ is found up to 373 K but, with increasing temperature, the behavior approaches an exponential distribution of $N(v_m^{-2})$. This crossover, which is in agreement with recent computer simulations of a ferroelastic switching process at different temperatures (compare e.g. with Fig. 2 of Ref.²⁸), is most probably due to thermal fluctuations at high temperatures that ease the motion of domain wall segments of various length l_i with a rate of $\tau(l_i)^{-1} = \tau_0^{-1} e^{-E(l_i)/T}$. On average, thermal fluctuations push the interface in the direction of the driving force and the average interface velocity is greater than zero even when the applied force F is smaller than the critical depinning force $F < F_c$. Indeed, Harrison et al.⁴ have shown that the maximum applied force required to unpin DW's in LaAlO_3 decreases drastically with increasing temperature from 800 mN at 370 K to 200 mN at 670 K.

5. Conclusions

In summary, the present work corroborates the physical picture that domain wall motion in ferroelastic materials involves various processes depending on temperature, time and spatial scale. By measuring real and imaginary parts of the dynamic Young's modulus as a function of temperature and frequency, the domain wall relaxation time τ_{DW} was determined. There are cases where τ_{DW} follows Arrhenius behavior (LaAlO_3) and where τ_{DW} follows Vogel-Fulcher behaviour (KDP, TGS, PbZrO_3). Probably systems closest to our investigated ferroelastic perovskites are ferroelastic-martensitic materials. In $\text{Ti}_{50-x}\text{Ni}_{50+x}$ strain glass behaviour has been reported for $x > 1$ ³⁴. The imaginary part of Young's modulus shows (for $x > 1$) a characteristic shift with frequency which can be fitted by assuming a Vogel-Fulcher dependence of the underlying relaxation time. In addition, the authors observed in HREM the appearance of uncorrelated nanodomains of ca. 1-5 nm size, which grow with decreasing temperature and get frozen at about 20-25 nm below T_g . Ren et al.³⁵ explained the observed strain glass behavior as a defect induced suppression of long range order, leading to the appearance of dynamic nanodomains whose dynamics freeze at T_g . Recently it was argued¹⁸ that in the case of ferroelastic materials domain boundary patterns can evolve glasslike states while the underlying matrix remains fully crystalline, without any defect induced disorder. Up to now, this concept of "Domain glass" is based on computer simulation results and although it is rather appealing, it seems not clear to us that any physical realization of a domain glass has yet been found experimentally for a real ferroelastic domain wall system. It is now clear that deviations from

an Arrhenius behaviour of domain wall dynamics have been detected for some ferroelastic systems, but the reasons for such deviations can be quite diverse. A Vogel-Fulcher dependence of the domain wall relaxation time is just one possibility, a temperature dependence of the distribution of relaxation times another. In our opinion, further experiments are required before a definite conclusion about the existence of domain glasses can be drawn.

6. Acknowledgments

The present work was supported by the Austrian Science Fund (FWF) Grant No. P28672-N36.

7. References

- Schranz W. Superelastic softening in perovskites. *Physical Review B*. 2011;83(9):094120.
- Schranz W, Kabelka H, Sarras A, Burock M. Giant domain wall response of highly twinned ferroelastic materials. *Applied Physics Letters*. 2012;101(14):141913.
- Kityk AV, Schranz W, Sondergeld P, Havlik D, Salje EKH, Scott JF. Low-frequency superelasticity and nonlinear elastic behavior of SrTiO₃ crystals. *Physical Review B*. 2000;61(2):946-956.
- Harrison RJ, Redfern SAT. The influence of transformation twins on the seismic-frequency elastic and anelastic properties of perovskite: dynamical mechanical analysis of single crystal LaAlO₃. *Physics of the Earth and Planetary Interiors*. 2002;134(3-4):253-272.
- Harrison RJ, Redfern SAT, Salje EKH. Dynamical excitation and anelastic relaxation of ferroelastic domain walls in LaAlO₃. *Physical Review B*. 2004;69(14):144101.
- Puchberger S, Soprunyuk V, Majchrowski A, Roleder K, Schranz W. Domain wall motion and precursor dynamics in PbZrO₃. *Physical Review B*. 2016;94(21):214101.
- Harrison RJ, Redfern SAT, Street J. The effect of transformation twins on the seismic-frequency mechanical properties of polycrystalline Ca_{1-x}Sr_xTiO₃ perovskite. *American Mineralogist*. 2003;88:574-582.
- Schranz W, Tröster A, Kityk AV, Sondergeld P, Salje EKH. Ultralow-frequency elastic response in Kmn_{1-x}Ca_xFe₃. *Europhysics Letters*. 2003;62(4):512-518.
- Schranz W, Sondergeld P, Kityk AV, Salje EKH. Dynamic elastic response of KMn_{1-x}Ca_xF₃: Elastic softening and domain freezing. *Physical Review B*. 2009;80(9):094110.
- Tagantsev AK, Cross LE, Fousek J. *Domains in Ferroic Crystals and Thin Films*. New York: Springer-Verlag; 2010.
- Sidorkin A. Dynamics of domain walls in ferroelectrics and ferroelastics. *Ferroelectrics*. 1997;191(1):109-128.
- Bornarel J, Torche B. Dielectric properties versus sample thickness in KH₂PO₄ ferroelectric crystals. *Ferroelectrics*. 1992;132(1):273-283.
- Huang YN, Li X, Ding Y, Shen H, Zhang ZF, Wang YN, et al. Domain Freezing in Triglycine Sulphate. *Le Journal de Physique IV*. 1996;6(C8):815-818.
- Huang YN, Li X, Ding Y, Wang YN, Shen HM, Zhang ZF, et al. Domain freezing in potassium dihydrogen phosphate, triglycine sulfate, and CuAlZnNi. *Physical Review B*. 1997;55(24):16159-16167.
- Kumar J, Awasthi AM. Glassy domain wall matter in KH₂PO₄ crystal: Field-induced transition. *Applied Physics Letters*. 2013;103(13):132903.
- Ren X, Wang Y, Otsuka K, Lloveras P, Castán T, Porta M, et al. Ferroelastic Nanostructures and Nanoscale Transitions: Ferroics with Point Defects. *MRS Bulletin*. 2009;34(11):838-846.
- Ren X. Strain glass and ferroic glass - Unusual properties from glassy nano-domains. *Physica Status Solid (b)*. 2014;251(10):1982-1992.
- Salje EKH, Ding X, Atkas O. Domain glass. *Physica Status Solid (b)*. 2014;251(10):2061-2066.
- Salje EKH, Carpenter MA. Domain glasses: Twin planes, Bloch lines, and Bloch points. *Physica Status Solid (b)*. 2015;252(12):2639-2648.
- Salje EKH, Ding X, Zhao Z, Lookman T, Saxena A. Thermally activated avalanches: Jamming and the progression of needle domains. *Physical Review B*. 2011;83(10):104109.
- Durin G, Zapperi S. The Barkhausen effect. In: Bertotti G, Mayergoyz I, eds. *The Science of Hysteresis*. Volume 2. Amsterdam: Elsevier; 2006. p. 181-267.
- Colaioni F. Exactly solvable model of avalanches dynamics for Barkhausen crackling noise. *Advances in Physics*. 2008;57(4):287-359.
- Durin G, Bohn F, Corrêa MA, Sommer RL, Le Doussal P, Wiese KJ. Quantitative Scaling of Magnetic Avalanches. *Physical Review Letters*. 2016;117(8):087201.
- Schranz W. Dynamic mechanical analysis-a powerful tool for the study of phase transitions. *Phase Transitions*. 1997;64(1-2):103-114.
- Salje EKH, Schranz W. Low amplitude, low frequency elastic measurements using Dynamic Mechanical Analyzer (DMA) spectroscopy. *Zeitschrift für Kristallographie*. 2011;226(1):1-17.
- Zhang Z, Koppensteiner J, Schranz W, Betts JB, Migliori A, Carpenter MA. Microstructure dynamics in orthorhombic perovskites. *Physical Review B*. 2010;82(1):014113.
- Redfern SAT, Wang C, Hong JW, Catalan G, Scott JF. Elastic and electrical anomalies at low-temperature phase transitions in BiFeO₃. *Journal of Physics: Condensed Matter*. 2008;20(45):452205.
- He X, Ding X, Sun J, Salje EKH. Parabolic temporal profiles of non-spanning avalanches and their importance for ferroic switching. *Applied Physics Letters*. 2016;108(7):072904.
- Tagantsev AK. Vogel-Fulcher relationship for the dielectric permittivity of relaxor ferroelectrics. *Physical Review Letters*. 1994;72(7):1100.

30. Calleja M, Dove MT, Salje EKH. Trapping of oxygen vacancies on twin walls of CaTiO_3 : a computer simulation study. *Journal of Physics: Condensed Matter*. 2003;15(14):2301.
31. Gonçalves-Ferreira L, Redfern SAT, Artacho E, Salje EKH, Lee WT. Trapping of oxygen vacancies in the twin walls of perovskite. *Physical Review B*. 2010;81(2):024109.
32. Rijal B, Delbreilh L, Saiter A. Dynamic Heterogeneity and Cooperative Length Scale at Dynamic Glass Transition in Glass Forming Liquids. *Macromolecules*. 2015;48(22):8219-8231.
33. Harrison RJ, Salje EKH. The noise of the needle: Avalanches of a single progressing needle domain in LaAlO_3 . *Applied Physics Letters*. 2010;97(2):021907.
34. Sarkar S, Ren X, Otsuka K. Evidence for strain glass in the ferroelastic-martensitic system $\text{Ti}(50-x)\text{Ni}(50+x)$. *Physical Review Letters*. 2005;95(20):205702.
35. Ren X, Wang Y, Zhou Y, Zhang Z, Wang D, Fan G, et al. Strain glass in ferroelastic systems: Premartensitic tweed versus strain glass. *Philosophical Magazine*. 2010;90(1-4):141-157.